Available online www.jsaer.com

Journal of Scientific and Engineering Research, 2017, 4(1):29-40

Research Article

ISSN: 2394-2630
CODEN(USA): JSERBR

Impact of irradiation on the surface recombination velocity of a back side monochromatic illuminated bifacial silicon solar cell under frequency modulation

Mouhamadou Mousliou DIALLO[1], Seni TAMBA[2], Boureima SEIBOU[3], Mohamed Lemine OULD CHEIKH[1], Ibrahima DIATTA[1], El Hadji NDIAYE[1], Youssou TRAORE[1], Cheikh Tidiane SARR[1], Gregoire SISSOKO[1]

[1]Laboratoire des Semi-conducteurs et d'Energie Solaire, Faculté des Sciences et Techniques, Université Cheikh Anta Diop, Dakar, Sénégal
[2]Ecole Polytechnique de Thiès, Thiès, Sénégal
[3]Ecole des Mines de Niamey Niger

Abstract In a dynamic frequency regime, the effect of irradiation on the bulk and surface recombination parameters (Sf, Sb) occurring in the bifacial photovoltaic cell monochromatically back-illuminated is presented. From the resolution of the continuity equation, through the photocurrent plots, we end with the expressions of Sf and Sb. Equivalent electric models related to Sf and Sb are deduced from Nyquist and Bode diagrams of the latter for some irradiation energy values. And subsequently, a method for determining equivalent electric parameters is proposed.

Keywords Irradiation-frequency modulation-recombination velocity-Bode and Nyquist diagram

1. Introduction

Solar cells are subject to a constant bombardment of high subatomic energy particles (electrons and protons). Thus, Electronic systems operating in space are exposed to radiation in the form of energetic charged particles, such as protons and heavy ions [1]. Indeed, irradiation of these cells generates atomic displacements within the material. Point defects resulting from these displacements trap the minority electric charge carriers produced by the illumination, which reduces the collection efficiency of the charges and alters the electrical characteristics of the cells (maximum power Pm, short circuit current J_{SC} and voltage in open circuit V_{OC}) [2]. Researchers have thus always carried out extensive studies in order to control and improve the behaviour of solar cells in such a hostile (irradiated) environment [3].

In this paper, the study deals with the impact of irradiation on the recombination parameters of a backside illuminated (BSI) bifacial photovoltaic cell under monochromatic light. First, we make a theoretical study to bring out all the mathematical equations for this type of photovoltaic cell. Then, using Nyquist and Bode diagrams [4-5], we put forward equivalent electrical model [6] for a few irradiation energy values. And in the end, a method for determining electric parameters relating to surface recombination velocities Sf and Sb will be proposed.

2. Theoretical Study

Our solar cell is made up of polycrystalline silicon [7-10], n^+-p-p+ type [11-12], with Back Surface Field (BSF) [13-14] whose structure is shown in the following figure.

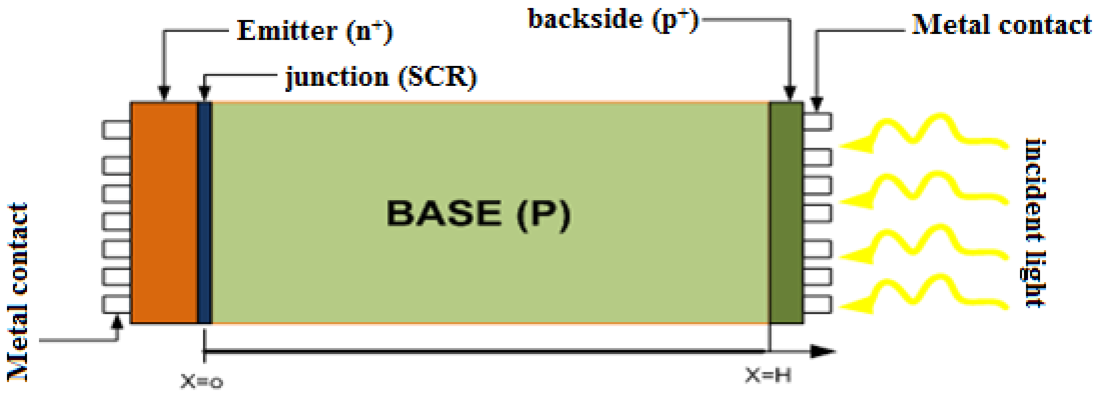

Figure 1: An n+-p-p+ structure of a silicon solar cell: backside illumination

This work is carried out with the assumptions that:

- ✓ the contribution of the emitter is neglected,
- ✓ the base is a quasi-neutral base (QNB)
- ✓ we use one-dimensional mathematical model. The origin is taken at the junction.

From these assumptions, the continuity equation is given in the following equation.

$$D(\kappa l,\phi).\frac{\partial^2\delta(x,t)}{\partial x^2}-\frac{\delta(x,t)}{\tau}=-G(x,t)+\frac{\partial\delta(x,t)}{\partial t} \qquad (1)$$

G (x, t) and δ (x, t) are respectively the global generation rate and the excess minority density carriers at position x and time t and can be written in the form as follows [15-19]:

$G(x, t) = g(x)e^{iwt}$ et $\delta(x,t) = \delta(x)e^{iwt}$ (2)

where, $g(x)$ and $\delta(x)$ typify the spatial components, $e^{i\omega t}$ the temporal component. Inserting equation (2) in equation (1) one obtains**:**

$$\frac{\partial^2\delta(x)}{\partial x^2}-\frac{1}{L(\omega,\kappa l,\phi)^2}\cdot\delta(x)=-\frac{g(x)}{D(\kappa l,\phi)} \qquad (3)$$

With,

$$\frac{1}{L^2(\omega,\kappa l,\phi)}=\frac{1}{L^2(\kappa l,\phi)}(i\omega\tau+1) \qquad \text{And} \qquad D(kl,\phi)=\frac{L^2(kl,\phi)}{\tau(kl,\phi)}$$

for this type of solar cell, the spatial component of the minority carrier generation rate is given by the expression (4):

$$g(x)=\alpha I_0(1-R)e^{-\alpha(H-x)} \qquad (4)$$

L_ω is the complex diffusion length [20]; α(λ) is the monochromatic optical absorption coefficient [21] at the wavelength λ; R (λ) is the reflection coefficient of the material at the wavelength λ; H the thickness of the base. D is the complex diffusion coefficient; ω is the angular frequency; τ is the average lifetime of the minority carriers obtained from the empirical relation as a function of the damage coefficient *kl* and the irradiation flux ϕ[22-23].

$$\frac{1}{\tau} = \frac{1}{\tau_0} + kl.\phi \tag{5}$$

The solution of the continuity equation is given by the following expression:

$$\delta(x) = A\cosh\left(\frac{x}{L_\omega}\right) + B\sinh\left(\frac{x}{L_\omega}\right) + \frac{\alpha.I_0.(1-R).L_\omega^{\ 2}}{D.(1-\alpha^2.L_\omega^{\ 2})}.\exp-\alpha(H-x) \tag{6}$$

Where coefficients A and B are to be determined from the boundary conditions at the junction and to the rear side **[24]**.

- At the Junction (x=0)

$$\left.\frac{\partial\delta(x)}{\partial x}\right)_{x=0} = S_f \cdot \frac{\delta(0)}{D} \tag{7}$$

- At the backside (x=H)

$$\left.\frac{\partial\delta(x)}{\partial x}\right)_{x=H} = -S_B \cdot \frac{\delta(H)}{D} \tag{8}$$

all calculation done, we get.

$$A_2 = \frac{\alpha.I_0.(1-R).L_\omega^{\ 3}\left\{-D.(\alpha.D+S_B)-(-\alpha.D+S_F)\left[D.\cosh\left(\frac{H}{L_\omega}\right)+L_\omega.S_B.\sinh\left(\frac{H}{L_\omega}\right)\right]e^{-\alpha H}\right\}}{D.(1-\alpha^2.L^2)\left[L_\omega.D(S_B+S_F).\cosh\left(\frac{H}{L_\omega}\right)+(D^2+S_F.S_B.L_\omega^{\ 2})\sinh\left(\frac{H}{L_\omega}\right)\right]} \tag{9}$$

$$B_2 = \frac{\alpha.I_0.(1-R).L_\omega^{\ 3}\left\{-L_\omega.S_F(\alpha.D+S_B)+(-\alpha.D+S_F)\left[D.\sinh\left(\frac{H}{L_\omega}\right)+L_\omega.S_B.\cosh\left(\frac{H}{L_\omega}\right)\right]e^{-\alpha H}\right\}}{D.(1-\alpha^2.L_\omega^{\ 2})\left[L_\omega.D(S_B+S_F).\cosh\left(\frac{H}{L_\omega}\right)+(D^2+S_F.S_B.L_\omega^{\ 2})\sinh\left(\frac{H}{L_\omega}\right)\right]} \tag{10}$$

Where S_f and S_B are respectively the recombination speed at the junction and to the rear side.

3. Photocourant Density

Knowing the expression of the minority density carriers, one can determine the expression of the photocurrent density by using the Fick law. It is given by the following equation:

$$J(Sf,Sb,\lambda,\omega,kl,\phi) = q.D.\left.\frac{\partial\delta(x,Sf,Sb,\lambda,\omega,kl,\phi)}{\partial x}\right|_{x=0} \tag{11}$$

all calculation done, we get:

$$Jph_2 = \frac{q.\alpha.I_o.(1-R).L^2}{(1-\alpha^2.L^2)}.\left\{\frac{-L.S_F.(S_B+\alpha.D)+.[L.\alpha.D(S_B+S_F)+.L.S_B.(S_F-\alpha.D)].\exp(-\alpha.H).\cosh\left(\frac{H}{L}\right)+[\alpha.(D^2+S_F.S_B.L^2)+D(S_F-\alpha.D)].\exp(-\alpha.H).\sinh\left(\frac{H}{L}\right)}{L.D(S_F+S_B)\cosh\left(\frac{H}{L}\right)+(D^2+S_F.S_B.L^2)\sinh\left(\frac{H}{L}\right)}\right\} \quad (12)$$

Where q is the charge of the electron and D the complex diffusion coefficient.

The photocurrent density according to the recombination velocity junction Sf_j and to backside Sb can be seen in figure 2.

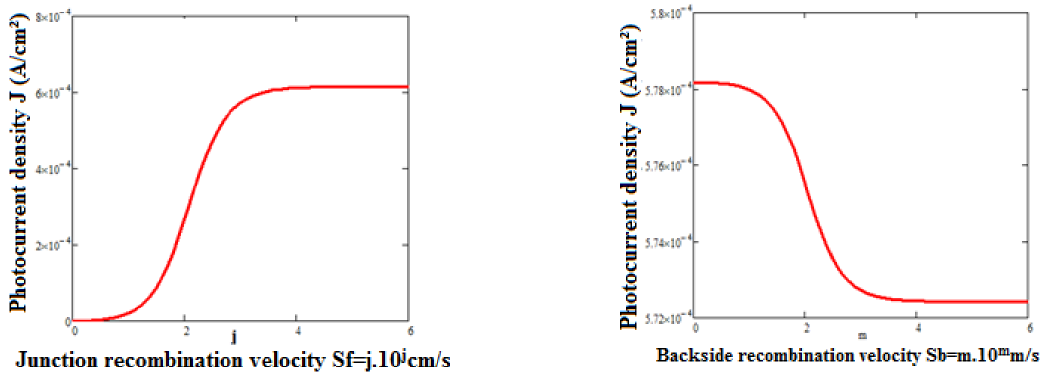

(a) **(b)**

Figure 2: Modulus of the photocurrent density versus the junction recombination velocity Sf_j (a) and the backside recombination velocity Sb_m (b)

$$\lambda = 0.98\mu\text{m} \ ; \ \omega = 10^6 \, rad/s \, ; \ kl = 15MeV^{-1}.s^{-1} \quad \phi = 150MeV$$

Plots of photocurrent density versus the recombination velocities (Sf and Sb) has a bearing for the high values of Sf ($Sf \geq 10^5$cm / s) and Sb ($Sb \geq 10^5$cm / s). Therefore, the zero gradient at that points lead to the expressions of the intrinsic recombination velocities through the junction and through the backside of the cell.

4. Expressions for Sf and Sb

Solving the equations (13) and (14) lead to the expressions of the recombination velocities Sf and Sb respectively [25-26].

$$\left[\frac{d[J_2(Sf, Sb, \lambda, \omega, \kappa l, \phi)]}{d[Sb(\lambda, \omega, \kappa l, \phi)]}\right]_{Sb \geq 10^5 cm/s} = 0 \quad (13)$$

$$\left[\frac{d[J_2(Sf, Sb, \lambda, \omega, \kappa l, \phi)]}{d[Sf(\lambda, \omega, \kappa l, \phi)]}\right]_{Sf \geq 10^5 cm/s} = 0 \quad (14)$$

After all calculation, one find:

$$Sf = \frac{D}{L_{\omega}} \times \frac{sh\left(\frac{H}{L_{\omega}}\right) + L_{\omega}\alpha\left(e^{-\alpha H} - ch\left(\frac{H}{L_{\omega}}\right)\right)}{L_{\omega}\alpha sh\left(\frac{H}{L_{\omega}}\right) - ch\left(\frac{H}{L_{\omega}}\right) + e^{-\alpha H}} \tag{15}$$

$$Sb = D \times \frac{\left(sh\left(\frac{H}{L_{\omega}}\right) + L_{\omega}\alpha ch\left(\frac{H}{L_{\omega}}\right)\right)e^{-\alpha H} - L_{\omega}\alpha}{\left(1 - ch\left(\frac{H}{L_{\omega}}\right) + L_{\omega}\alpha \times sh\left(\frac{H}{L_{\omega}}\right)\right) \times e^{-\alpha H} L_{\omega}} \tag{16}$$

5. Bode and Nyquist Plots Relating to Sb and Sb

The Bode and Nyquist plots [27-29] are used here to evaluate the impact of irradiation on the recombination velocities. And also, to describe the electrical phenomena of the intrinsic recombination velocities at the Junction Sf and to the backside Sb.

5.1. Bode Plots

Plots Bellow illustrate how the irradiation energy affect the recombination parameters.

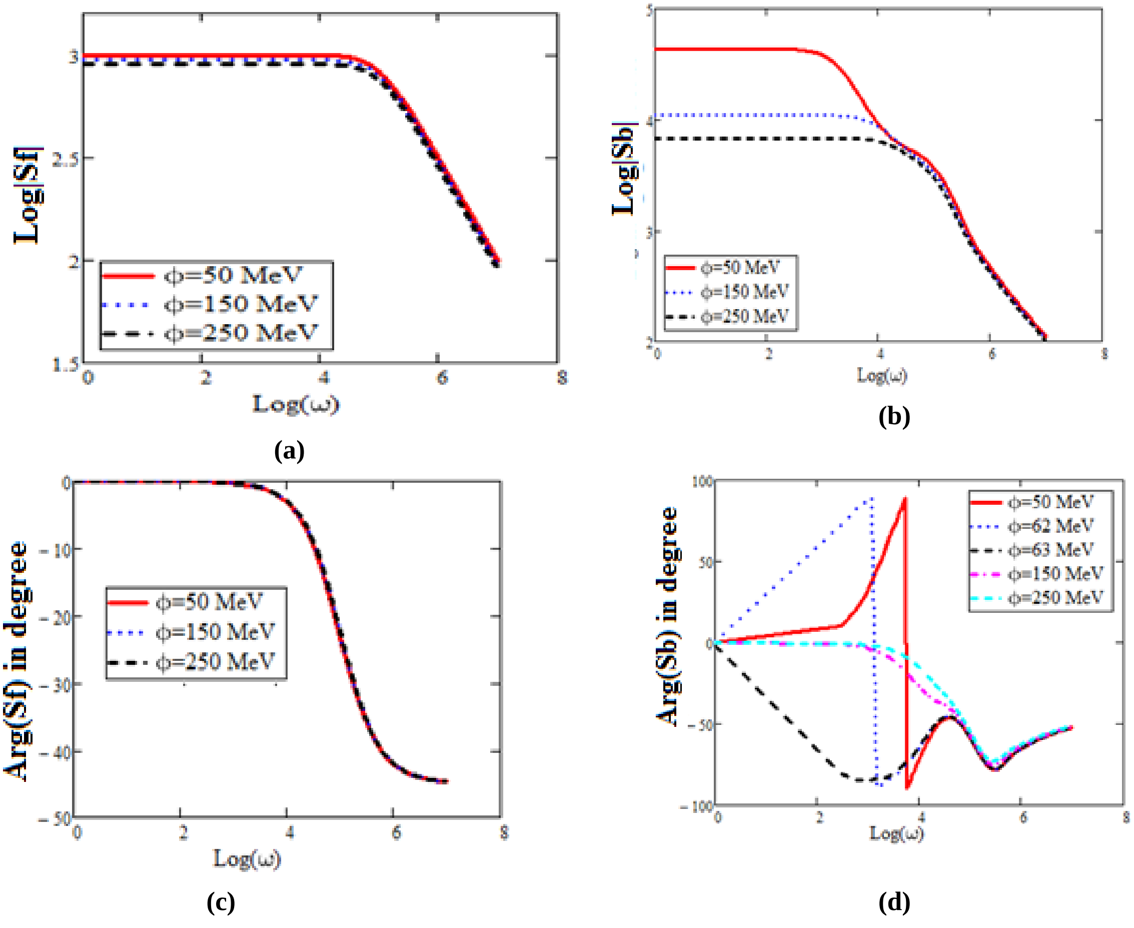

Figure 3: Bode plots for various irradiation values $\lambda = 0.98\mu\text{m}$; $kl = 15 MeV^{-1}.s^{-1}$

Plots (a) and (b) show that the modulus of recombination velocities (Sf and Sb) is insensitive to the angular frequency as long as the latter is less than the quasi-static cut-off pulsation ωc, and beyond this pulsation, the modulus of Sb and Sf, very sensitive to the frequency, decreases abruptly according to the pulsation (dynamic frequency regime). High frequencies lead to small values of the recombination velocities, thus less losses of minority carriers at the emitter-base and at the backside. Moreover, the effect of irradiation is more perceptible when operating in quasi-static regime and the more it increases, less important the recombination. Furthermore, the increase in irradiation results in an increase in the value of the cut-off frequency (boundary frequency between the quasi-static regime and the dynamic frequency regime, fig.a).

Figure (d) shows:

- For any given irradiation energy greater than or equal to 63 MeV, there is a pulsation below which the phase of the recombination velocity is nil. Beyond that pulsation, the phase decreases and remains negative so as to materialize a predominance of capacitive effects over inductive effects.
- For any irradiation energy, less than or equal to 62 MeV, the phase of the recombination velocity remains positive nearby the resonance and then becomes negative for higher frequencies: this describes both the inductive and capacitive phenomena of the backside recombination velocity.

The graph (c), shows that, regardless of the applied irradiation energy, there's always a predominantly capacitive effect.

5.2. Nyquist Plots for Sf and Sb

The impact of irradiation on the Nyquist plots is shown in the graphs below

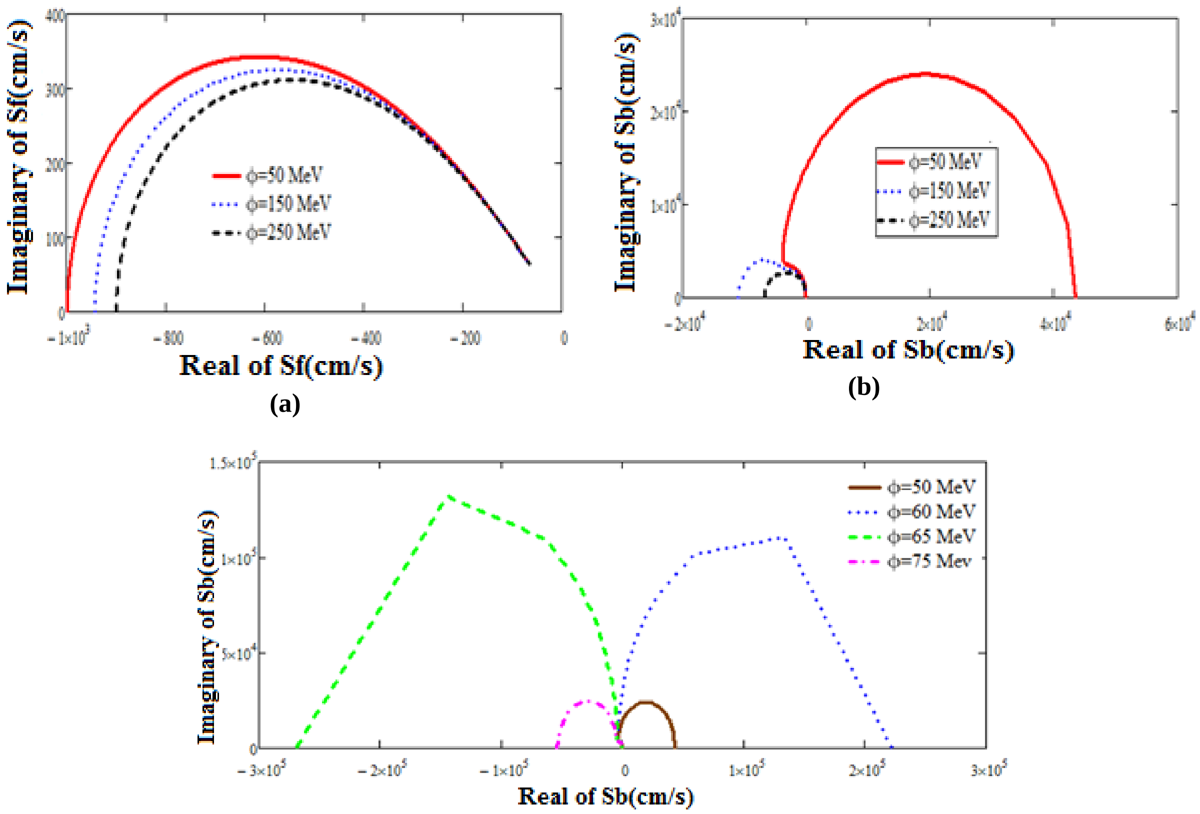

(a) **(b)**

(c)

Figure 4: Nyquist plots for Sf (a) and for Sb (b, c) for various irradiation energy values $\lambda = 0.98\mu\text{m}$;

$$kl = 15MeV^{-1}.s^{-1}$$

On these plots, you can see that they all are semi-closed loop curves of variable diameters depending on the value of the irradiation. Indeed, the greater the energy the greater the radius, characterizing both the capacitive and inductive phenomena of the recombination velocities Sb and Sf.

In concordance with the Bode diagram of Figure 3 (d), one can notice see that there is an energy above which the capacitive effects predominate over the inductive effects and below which these two effects coexist (Figure c).

6. Equivalent Electrical Circuit Model for an Irradiation Energy Equal to 50 MeV

Based on the Nyquist and Bode plots, some equivalent electric models for the recombination velocities Sf and Sb at Φ=50 MeV are proposed. And subsequently, a graphical method for determining equivalent electric parameters will be proposed too.

6.1. Junction Recombination Velocity Sf

An electrical circuit can be proposed based on the imaginary part of the junction recombination velocity vs its real part (see table 1

Table 1: equivalent electric circuit of Sf; $\lambda = 0.98\mu\text{m}$; $kl = 15MeV^{-1}.s^{-1}$

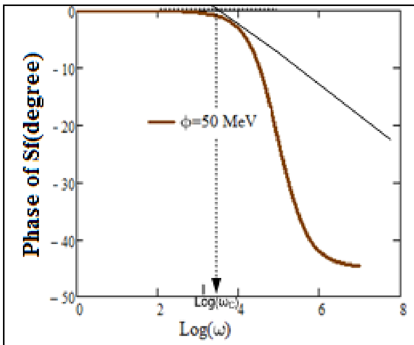

(a)

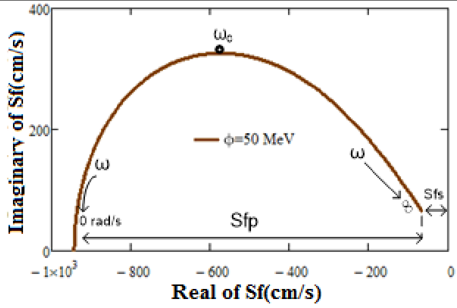

(b)

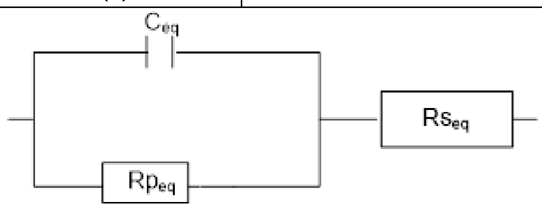

(c)

The storage, the losses due to the recombination of the excess minority carriers through the emitter-base interface, can be electrically designed by a capacitance C, a shunt resistor Rp and a series resistance Rs respectively.

The equivalent electrical circuit (c) describes the electric behaviour of the recombination velocity through the junction Sf. The losses due to the recombination of the carriers through the emitter-base are assimilated to resistors.

C_{eq} is the capacitance of a capacitor which characterizes the capacitive effects of the recombination velocity Sf; Rp_{eq}, is a shunt resistance and Rs_{eq} is a series resistance. The values of the series resistance Rs_{eq} ($\omega \to 0$ or $\omega \to \infty$), shunt Rp_{eq}, (from the cut-off frequency giving Rpéq / 2) can be evaluated using diagram (b). Knowing the value of the cut-off frequency, we can be deduced the value of the photogenerated minority carriers' lifetime and the capacitance from the relations $\tau = 1/\omega_c$ et $\tau = Rp_{eq}.C_{eq}$ [30-31].

6.2. Backside Recombination Velocity Sb

An electric circuit can be proposed based on the imaginary part of the backside recombination velocity vs its real part (see table 2).

Table 2: equivalent electric circuit method for Sb $\lambda = 0.98\mu\text{m}$; $kl = 15MeV^{-1}.s^{-1}$

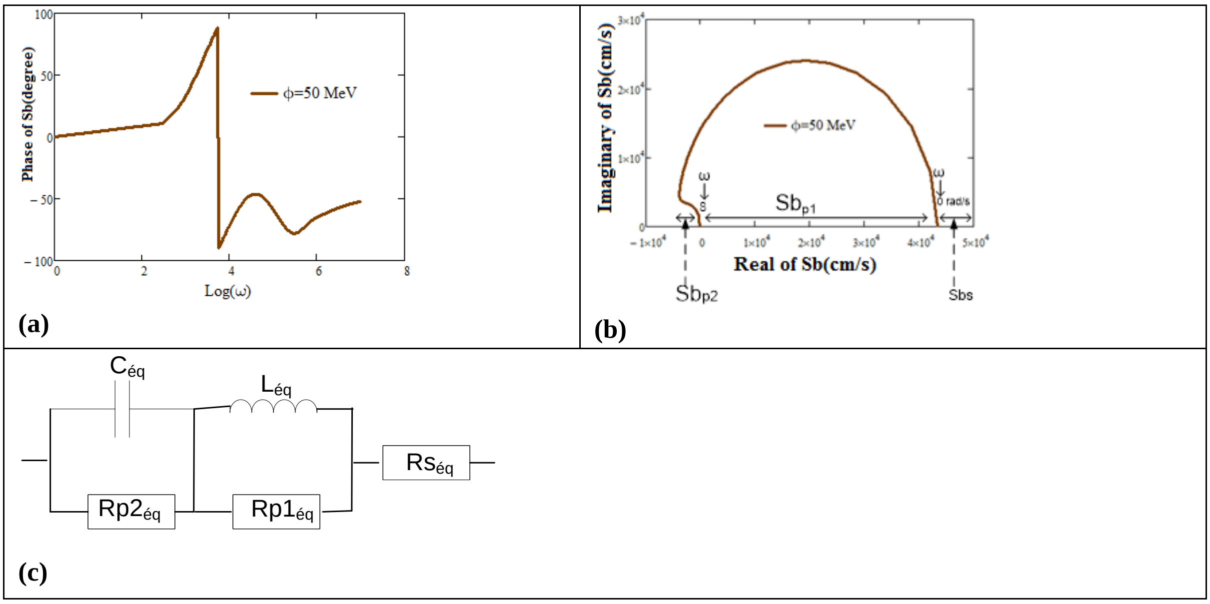

Using the Nyquist plot (b), the equivalent electrical circuit (c) of the table2 describes the capacitive and inductive phenomena observed from the phase of Sb (a). Ceq represents the capacitive effects and Leq the inductive effects. $Rp1_{eq}$ is a shunt resistance estimated when the excitation pulse $\omega \rightarrow 0$ and $\omega \rightarrow \infty$ .and Rp2eq a shunt resistance corresponding to the diameter of the semicircle of the capacitive phenomenon.

We note that $Rp2_{eq}$ is less than $Rp1_{eq}$ but still when $Rp2_{eq}$ is zero, the inductive effects prevail. It is the same when the pulsation $\omega<10^3$ rad / s. And in this frequency domain, the imaginary of Sb vs the logarithm of the pulsation is a straight line whose slope represents the equivalent inductance Leq (diagram c).

6.3. Graphical method for determination of electric parameters (Rs_{eq}, Rp_{eq} and L_{eq})

The method consists of representing the modulus of the series and shunt resistances vs the real part of Sf (or Sb). For each value of Sfp or Sfs (Sbs or Sbp) obtained, we proceed its projection on the curves then the y-intercepts (modulus of Rseries or Rshunt) give the values of Rs_{eq} or Rp_{eq}.

Whereas the slope of the imaginary of Sb vs the pulsation (ω<103) graph (c) (Table 3) gives the equivalent inductance Leq, graph (c) Table 2.

Example: recombination velocity Sf

Table 3: evaluation method of electric parameters (Rs_{eq}, Rp_{eq} and L_{eq})

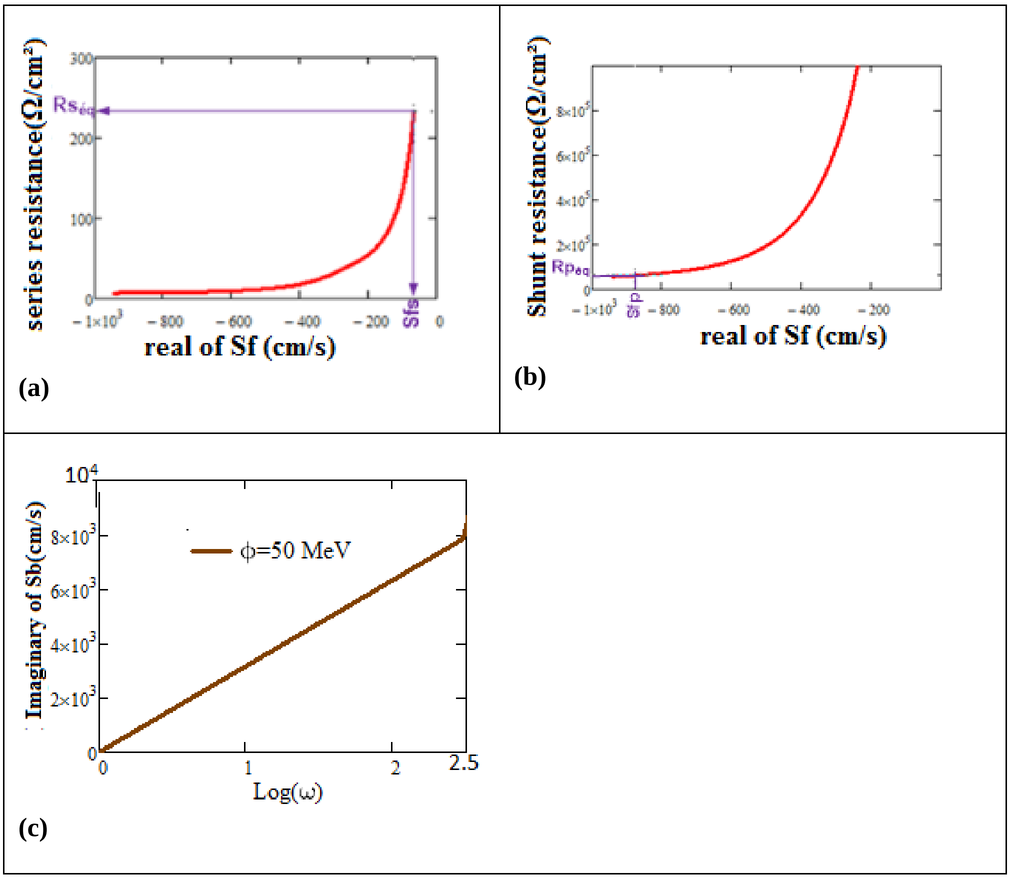

For each value of Sfs or Sfp obtained from the Nyquist plot (Table 1) there is corresponding value of Rs_{eq} or Rp_{eq}. Indeed:

- The diameter of the semicircle Sfp (diagrams b, Table 1) lead to the shunt resistance Rp_{eq} (diagram c, table 1);
- Sfs, determined when $\omega \rightarrow 0$ or $\omega \rightarrow \infty$, lead to the equivalent series resistance Rs_{eq} (graph c Table 1).

Knowing the value of the cut-off frequency, we can deduce the equivalent electrical capacitance from the equation $\tau = 1/\omega_c$ et $\tau = Rp_{eq}.C_{eq}$.

The table 4 below gives values of the parameters mentioned above for three (3) irradiation energy values.

Table 4: values of Electric parameters

Φ(MeV)	**|Sfs|(cm/s)**	**|Sfp| (cm/s)**	**$Rs_{éq}$(Ω/cm²)**	**$Rp_{éq}$(Ω/cm²)**	**$C_{éq}$(µF/cm²)**
50	69,314	993,086	13,988	13562	$2,331.10^{-2}$
150	66,392	926,71	14,964	15066	$2,099.10^{-2}$
250	64,055	874,825	15,866	16517	$1,914.10^{-2}$

when the irradiation energy values increase, the resistances Rs_{eq} and Rp_{eq} increase whereas the equivalent electrical capacitance decreases. This is due to the fact that the irradiation damages the material causing an increase in losses of minority carriers. The intrinsic properties of the solar cell are damaged; Resulting in poor cell quality.

The decrease of the capacitance was predictable since the capacitance is inversely proportional to the shunt resistance (which increases) according to the expression $C_{eq} = 1 / (Rp_{eq} * \omega c)$. In fact, the diffusion capacitance decreases since there are few of minority carriers diffusing in volume [32-33].

7. Conclusion

The recombination velocities of the bifacial silicon solar cell are very sensitive to the irradiation energy. Indeed, an increase in irradiation causes more losses of minority carriers. The negative impact of irradiation particles is more accentuated for the greater energy values. Then it is clear that even with the low values of energy, for a prolonged exposure to irradiations, the damage resulting from the impact of irradiation will be significant.

References

[1]. Dale McMorrow, Stephen Buchner, and Jonathan Pellish, "Single-Event Effects in Microelectronics Induced by Through-Wafer Sub-Bandgap Two-Photon Absorption"; Proceedings of 10th international workshop on radiation effects on semiconductor devices for space application, JAXA-SP. pp 110-114 (march 2013).

[2]. A.Ibrahim. "Analysis of electrical characteristics of photovoltaic single crystal silicon solar cells at outdoor measurements". Smart grid and renewable energy, vol.2 No.2, pp169-175, (2011)

[3]. Kayali, S; McAlpine, W.; Becker, H.; Scheick, L., "Juno radiation design and implementation," Aerospace Conference, 2012 IEEE, pp.1-7, 3-10 March 2012

[4]. R. Anil Kumar, M.S. Suresh and J. Nagaraju. "Measurement of AC parameters of Gallium Arsenide (GaAs/Ge) solar cell by impedance spectroscopy", IEEE Transactions on Electron Devices, Vol.48, No.9, pp 2177-2179, September 2001.

[5]. El Hadji NDIAYE, Gokhan SAHIN, Moustapha DIENG, Amary THIAM, Hawa LY DIALLO, Mor NDIAYE, Grégoire SISSOKO "Study of the intrinsic recombination velocity at the junction of silicon solar cell under frequency modulation and radiation" Journal of Applied Mathematics and Physics, 2015, 3,1522-1535 Published Online November 2015 in SciRes. http://www.scirp.org/journal/jamp http://dx.doi.org/10.4236/jamp.2015.311177.

[6]. A Dieng, I. Zerbo, M. Wade, A. S. Maiga and G. Sissoko. "Three-dimensional study of a polycrystalline silicon solar cell: the influence of the applied magnetic field on the electrical parameters". Semicond. Sci. Technol. 26; 095-023; (2011).

[7]. N. Bordin, L. Kreinin, N. Eisenberg. "Determination of recombination parameters of bifacial silicon cells with a two layer step-liked effect distribution in the base region" Proc.17th European PVSEC, pp.1495-1498, (Munich, 2001)

[8]. Wiley and Sons "Solar Electricity" John University of Southampton UK. pp.228, 1994

[9]. Keith R. Mclntosh, Christiana B. Honsberg, Stuart R. Wenham. "The impact of rear illumination on bifacial solar cells with floating junction passivation," in Proc. 15th EC PVSEC, pp. 1515–1518 (1998)

[10]. P. Yadav, K. Pandey, B. Tripathi, C. M. Kumar, S. K. Srivastava, P.K. Singh, M. Kumar, "An effective way to analyse the performance limiting parameters of poly-crystalline silicon solar cell fabricated in the production line", Solar Energy 122 (2015) 1–10.

[11]. Hübner, A., Aberle, A.G. and Hezel, R. "20% Efficient Bifacial Silicon Solar Cells". 14th European Photovoltaic Solar Energy Conference, 1796-1798, Munich, 2001.

[12]. Meier, D.L., Hwang, J.-M. and Campbell, R.B "The Effect of Doping Density and Injection Level on Minority Carrier Lifetime as Applied to Bifacial Dendritic Web Silicon Solar Cells". IEEE Transactions on Electron Devices, ED-35: pp 70-79 (1988)

[13]. A. Schneider, C. Gerhards, F. Huster, W. Neu, M. Spiegel, P. Fath, E. Bucher, R.J.S. Young, A.G. Prince, J.A. Raby, A.F. Caroll. AL "BSF for thin screen-printed multicrystalline Si Solar Cells". Proc.17th European PVSEC, pp 1768 – 1771, (Munich,2001)

[14]. David Bertrand; Sylvain Manuel; Marc Pirot; Anne Kaminski-Cachopo; Yannick Veschetti "Modelling of Edge Losses in Al-BSF Silicon Solar Cells", IEEE Journal of Photovoltaics, Vol. 7, pp 78 – 84, 2017

[15]. Sudha Gupta, Feroz Ahmed and Suresh Garg. "A method for the determination of the material parameters τ, D, L_o, S and α from measured A.C. short-circuit photocurrent Solar Cells, Vol. 25, pp 61-72, (1988)
[16]. J.N. Hollenhorst, and G. Hasnain. "Frequency dependent hole diffusion in I_nGaAs double heterostructures" Appl. Phys. Lett. Vol.67 (15), (1995) pp 2203 – 2205
[17]. Luc Bousse, Shahriar Mostarshed and Dafeman. "Investigation of Carrier Transport Through Silicon Wafers by Photocurrent Measurements". J. Appl. Phys. Vol.75 (8), (1994),pp4000-4008
[18]. T. Flohr and R. Helbig, "Determination of minority-carrier lifetime and surface recombination velocity by Optical-Beam-Induced-Current measurements at different light wavelengths," J. Appl. Phys., vol. 66, iss.7, pp. 3060-3065, 1989.
[19]. José Furlan and Slavko Amon. "Approximation of the carrier generation rate in illuminated silicon" Solid state Electric. Vol. 28, N° 12 pp.1241-1243
[20]. A. Mandelis. Coupled ac. Photocurrent and photothermal reflectance response theory of semiconducting p-n junctions J. Appl. Phys. Vol.66 (11), pp 5572 – 5583, (1989).
[21]. G. Sissoko, C. Musereka, A. Correrea, I. Gaye, A. L. Ndiaye. "Light spectral effect on recombination parameters of silicon solar cell". Proc. World Renewable Energy Congress 15-21 June Denver- USA, part III, pp 1487-1490, (1996).
[22]. M.A. Ould El Moujtaba, M. Ndiaye, A.Diao, M.Thiame, I.F. Barro and G. Sissoko. Theoretical Study of the Influence of Irradiation on a Silicon Solar Cell under Multispectral Illumination. *Res. J. Appl. Sci. Eng. Technol., 4(23): 5068-5073, 2012*
[23]. I. Ly, M. Wade, H. Ly Diallo, M.A. El Moujitaba, O.H. Lemrabott, S. Mbodj, O. Diasse, A. Ndiaye, I. Gueye, F.I. Barro, A. Wereme, G. Sissoko. Irradiation Effect on the Electrical Parameters of a Bifacial Silicon Solar Cell under Multispectral Illumination : 26ème Conférence Européenne sur l'Energie Solaire Photovoltaïque (26th EU PVSEC), pp.785-788(2011).
[24]. G. Sissoko, C. Museruka, A. Corréa, I. Gaye, A. L. Ndiaye. "Light spectral effect on recombination parameters of silicon solar cell", World Renewable Energy Congress, part III, pp.1487-1490, (1996)
[25]. Y. L. B. Bocande, A. Correa, I. Gaye, M. L. Sow and G. Sissoko. Bulk and surfaces parameters determination in high efficiency Si solar cells. Renewable Energy, vol 5, part III, pp. 1698-1700, 1994-Pergamon, 0960-1481 / 94$ 700 +0.00
[26]. Diallo. H.L., A.S. Maiga, A. Wereme and G. Sissoko, "New approach of both junction and back surface recombination velocities in a 3D modelling study of a polycrystalline silicon solar cell", Eur.Phys. J. Appl. Phys., 42, pp. 203- 211 (2008).
[27]. H. Ly Diallo, M. Wade, I. Ly, M. NDiaye, B. Dieng, O.H. Lemrabott, A.S. Maïga and G. Sissoko "1D Modeling of a Bifacial Silicon Solar Cell under Frequency Modulation, Monochromatic Illumination: Determination of the Equivalent Electrical Circuit Related to the Surface Recombination Velocity Research" Journal of Applied Sciences, Engineering and Technology (4)1672-1676, (2012).
[28]. I. Gaye, A. Corréa, A. L. Ndiaye, E. Nanéma, M. Adj, G. Sissoko."Impedance parameters determinati on of silicon solar cell using the one diode model in transient study". Renewable Energy, Vol 3, pp. 1598-1601, 1996.
[29]. Lathi, Bhagwandas Pannalal. "Signals, systems and controls" In-text Educational Publisher, New York, 1973-1974
[30]. R.A. Sinton, A. Cuevas, "Contactless determination of current–voltage characteristics and minority-carrier lifetimes in semiconductors from quasi-steady-state photoconductance data", Applied Physics Letters 69 ,2510–2512, (1996)
[31]. G. Garcia-Belmonte ET AL. "Simultaneous determination of carrier lifetime and electron density-of-states in P3HT: PCBM organic solar cells under illumination by impedance spectroscopy" Solar Energy Materials & Solar Cells 94 (2010) 366–375.
[32]. Amadou Diao, Ndeye Thiam, Martial Zoungrana, Gokhan Sahin, Mor Ndiaye, Grégoire Sissoko. "Diffusion Coefficient in Silicon Solar Cell with Applied Magnetic Field and under Frequency: Electric Equivalent Circuits'' World Journal of Condensed Matter Physics, 4, pp 84-92, (2014).

[33]. Gokhan Sahin, Moustapha Dieng, Mohamed Abderrahim Ould El Moujtaba Moussa Ibra Ngom, Amary Thiam, Grégoire Sissoko. “Capacitance of Vertical Parallel Junction Silicon Solar Cell under Monochromatic Modulated Illumination” Journal of Applied Mathematics and Physics, 2015, 3, 1536-1543. Published Online November 2015 in SciRes. http://www.scirp.org/journal/jamphttp://dx.doi.org/10.4236/jamp.2015.311178.